3Pa2-5

Investigation on Shape of Driving Signal to Improve Results of Reflection Point Search using Rectangular Sound Source

Hiroyuki Masuyama† (NIT, Toba College)

1. Introduction

Rectangular ultrasonic transducers have four vertices and four sides, and a spatial impulse response of them changes complicatedly depending on the order in which edge waves from these vertices and sides and direct waves from the sound source surface arrive at the observation point[1]. In addition, the waveform acquired by a rectangular sound source changes depending on the position of the observation point. A method to apply this complicated change to the reflection point search using a single rectangular sound source[2-5] or a rectangular array sound source with a small number of elements[6-8] has been proposed.

In this study, an investigation on the shape of the driving signal of the sound source is conducted. To search for reflection points, the cross-correlation between the acquired reflected signal and the reflected signals obtained by calculations is used. The desired driving signals of the sound source are those in which the cross-correlation coefficients appear sharply. Using such driving signals is expected to improve the search results. As a driving signal of the sound source that can be generated relatively concise for conducting experiments, a signal based on a single-frequency burst wave with code modulation will be investigated. The validity of the investigation result is confirmed by performing numerical calculations.

2. Method of Reflection Point Search

The configuration of a rectangular sound source and a reflection point P is shown in **Fig. 1**. The position of the reflection point is indicated by $P(\boldsymbol{r})$. In the calculation result showing in the following section, $\boldsymbol{r}$ is expressed using the distance from the origin of the coordinates ($|\boldsymbol{r}|$), the azimuth angle, and the elevation angle.

When the sound source is driven with uniform velocity $v(t)$, and when the wave radiated from the sound source is reflected at P, the output $e(\boldsymbol{r}, t)$ in terms of the reflected wave received at the sound source is expressed as[9]

$$e(\boldsymbol{r},t) = -\frac{k\rho A}{2c} v(t) * \frac{\partial}{\partial t} h(\boldsymbol{r},t) * \frac{\partial}{\partial t} h(\boldsymbol{r},t), \quad (1)$$

where k is the proportionality constant, ρ is the density of the propagation medium of the sound wave, A is the area of the region in which the reflection point contributes to the reflection, c is the velocity of sound, $h(\cdot)$ is the spatial impulse response of the sound source, and $*$ denotes the convolution integral.

The procedure diagram for searching for reflection points and obtaining search results is also shown in Fig. 1. Since the rise time of the reflected wave is measurable, the value of $|\boldsymbol{r}|$ can be determined in the range expressed as

$$\frac{cT}{2} \le |\boldsymbol{r}| \le \frac{cT}{2} + \sqrt{a^2 + b^2}, \quad (2)$$

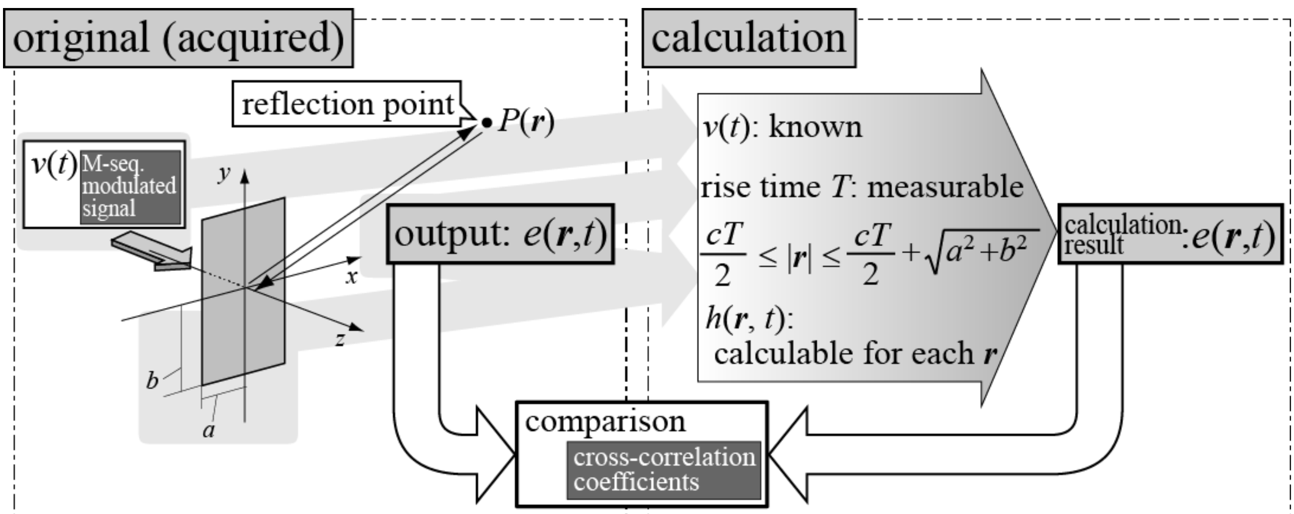

Fig. 1 Configuration of a sound source with a rectangular element and a reflection point P, and the procedure diagram for searching reflection points and obtaining search results.

e-mail address: masuyama@toba-cmt.ac.jp

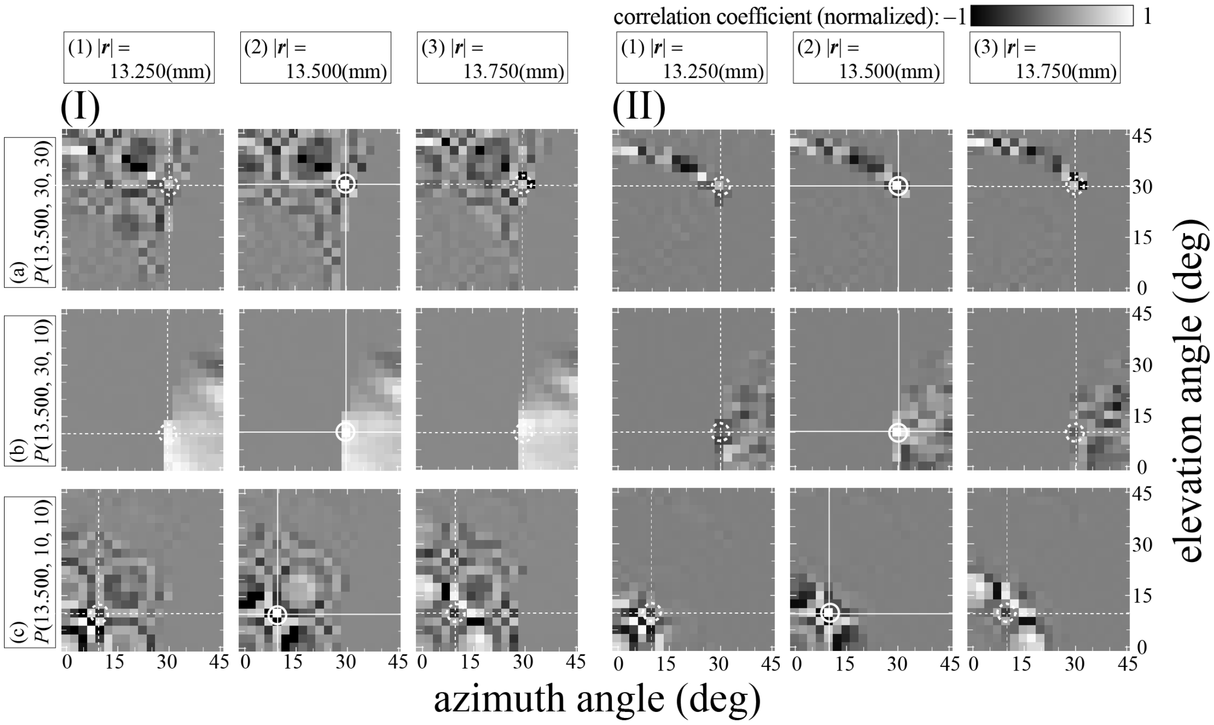

Fig. 2 Calculation results of cross-correlation coefficients using single rectangular sound source at three reflection points: (I) using signal for driving sound source modulated with M-sequence code; (II) using non-modulated signal for driving sound source.

where T is the rise time of the reflected wave, and c is velocity of sound. When the value of $\boldsymbol{r}$ is set at an appropriate interval in the range of $|\boldsymbol{r}|$, the spatial impulse response $h(\boldsymbol{r}, t)$ corresponding to each $\boldsymbol{r}$ can be obtained. Since $v(t)$ is known, the output waveform $e(\boldsymbol{r}, t)$ in eq. (1) at each $\boldsymbol{r}$ can be calculated. By deducing the cross-correlation coefficient between the waveform obtained by the calculation and the original (acquired) reflected wave in the sequential order, it becomes possible to estimate the position of the reflection point P.

3. Numerical Calculations

The results of numerical calculations by the sound source with a rectangular element are shown in **Fig. 2**. The results are obtained by calculating convolution integral in eq. (1) and the cross-correlation coefficient at time zero with the calculation result for the points around the reflection points sequentially. The dimensions of the sound source used in the calculation are a = 6.450 mm, and b = 10.050 mm. The driving signal for the sound source $v(t)$ is a burst wave with a driving frequency of 3 MHz and a duration interval of 14 cycles, modulated every two cycles with a third-order M-sequence code.

In Fig. 2(I), calculation results of the cross-correlation coefficients for each set reflection point P using the modulated signal described above as the driving signal of the sound source are shown. For the comparison, the results when the conventional non-modulated signal is used as the driving signal for the sound source are also shown in Fig. 2(II). In Fig. 2(I), the conspicuous striped patterns appearing in the conventional search results shown in Fig. 2(II) are slightly less noticeable and milder. However, in Fig. 2(I), the area of blurred stripes indicating small variations in cross-correlation coefficient values is expanded compared to Fig. 2(II).

4. Summary

In order to improve the search results for reflection points using the rectangular sound source, an investigation on the driving signal of the sound source was conducted. A signal based on a single frequency burst wave with code modulation was investigated as the driving signal for the sound source. Calculation results showed a slight improvement compared to conventional search results. Further investigation is needed on the method of configuring sound source driving signals to improve the search results.

References

1. J. L. San Emeterio and L. G. Ullate: J. Acoust. Soc. Am. **92** (1992) 651.
2. H. Masuyama and K. Mizutani: Jpn. J. Appl. Phys. **46** (2007) 7793.
3. H. Masuyama: Proc. Symp. USE **38** (2017) 1P2-5.
4. H. Masuyama: Proc. Symp. USE **41** (2020) 3Pb2-4.
5. H. Masuyama: Proc. Symp. USE **42** (2021) 1Pb2-7.
6. H. Masuyama and K. Mizutani: Jpn. J. Appl. Phys. **48** (2009) 07GC05.
7. H. Masuyama: Proc. Symp. USE **39** (2018) 1P2-9.
8. H. Masuyama: Proc. Symp. USE **40** (2019) 1P2-4.
9. J. P. Weight and A. J. Hayman: J. Acoust. Soc. Am. **63** (1978) 396.